

MWCNTs-Supported Pd(II) Complexes with High Catalytic Efficiency in Oxygen Reduction Reaction in Alkaline Media.

Maurizio Passaponti,^{‡a} Matteo Savastano,^{‡a,b} M. Paz Clares,^c Mario Inclán,^c Alessandro Lavacchi,^d Antonio Bianchi,^{*a} Enrique García-España^{*c} and Massimo Innocenti.^{*a}

^a Department of Chemistry “Ugo Schiff”, University of Florence, via della Lastruccia 3, 50019 Sesto Fiorentino, Italy.

^b CSGI, University of Florence, via della Lastruccia 3, 50019 Sesto Fiorentino, Italy.

^c Supramolecular Chemistry Group, Institute of Molecular Sciences, University of Valencia, 46980 Paterna, Spain.

^d ICCOM-CNR, via Madonna del Piano 10, 50019 Sesto Fiorentino, Italy.

Supporting Information Placeholder

ABSTRACT: We report here the remarkable catalytic efficiency observed for two Pd(II) azamacrocyclic complexes supported on MWCNTs towards ORR. Beyond a main (>90%) 4 e⁻ process and onset potential close to or better than those of commercial Pt-electrodes, the multi-walled carbon nanotubes (MWCNTs) functionalization strategy, aiming at chemically defined Pd(II)-based catalytic centers, allowed the half-cell to exceed PEM fuel cell reference/target mass activity efficiency set by US Department of Energy (DOE) for 2020 (440 mA/mg_{PGM} at 0.9 V vs Reversible Hydrogen Electrode (RHE)).

Fuel cells are promising candidates for sustainable future energetic technology. Oxygen reduction reaction (ORR) allows to release the chemical energy stored in the vector molecule H₂ in the form of electrical work without producing any waste but innocuous H₂O molecules. For this reason, oxygen reduction is regarded as a highly strategic reaction, upon whose efficiency the near-future energy storage and powering technology depend.

The use of cathode catalyst is mandatory to achieve satisfying ORR conversion rate. Although many efforts have been made, and several Carbon-based nanomaterials have been assessed, Pt-based catalysts remains unchallenged as of today in terms of produced current density (J), low onset potential (E_{on}) and avoidance of production of the reactive H₂O₂, rather favoring direct conversion to H₂O.¹ As Pt and the so-called Platinum Group Metals (PGM) are rare and expensive –one of the key unsolved issues for the widespread use of fuel cells– much research effort has been oriented to reduce the required amount of metal to reach the desired performances.²⁻⁶ As the useful timespan for the replacement of fossil fuels narrows, international protocols and agreements with specific objectives and deadlines are stipulated. The upcoming 2020 efficiency goal for fuel cells was expressed in this same spirit, i.e. in terms of mass activity, by the US DOE, requiring that a threshold current is produced per quantity of PGM under certain conditions (440 mA/mg_{PGM} at 0.9 V vs RHE) in acidic media.⁷

Herein we report a hydrodynamic study on the half-cell, as it is best practice for benchmarking ORR catalysts performances,^{8,9} conducted on two novel Pd(II)-based catalysts in alkaline solutions, as Pt-free alkaline fuel cells were recently proved¹⁰⁻¹² to be efficient in delivering stable performances and power density above 1 W cm⁻². One of our new catalyst exceeds target mass ac-

tivity value by over 10%, featuring an E_{on} identical or better than that of a Pt electrode (0.91 V vs RHE) and an almost exclusive (96.5% at 0.9 V vs RHE) 4 e⁻ process, i.e. promoting selectively the direct conversion of O₂ to H₂O (see Table 1). Such features were made possible by the supramolecular architecture of our supported catalysts, enabling the homogeneous distribution on MWCNTs of the Pd(II) complexes, without disrupting neither the nanostructured nature of substrate nor its π-delocalized system.

The catalysts, MWCNT/HL1-Pd(II) and MWCNT/HL2-Pd(II), evaluated in this work (Figure 1) were obtained through a supramolecular approach. High purity (99.9% C) graphitized MWCNTs were chosen as a substrate, both in view of the usefulness of nanostructured carbon in catalysis and for their unspoiled electrical properties.¹³ Their non-covalent functionalization with either HL1 or HL2 (Figure 1) by spontaneous chemisorption in water according to previously described procedures,^{14,15} afforded the MWCNT/HL1 and MWCNT/HL2 hybrid materials, without disrupting the delocalized π electron systems of the CNTs. Adsorption of HL1, HL2 and analogous pyrimidine derivatives on graphitic surfaces from aqueous solutions has been previously reported to happen mainly through the electron-deficient pyrimidine residue, rather than involving the protonated amine chain, as water actively competes for the ammonium groups.¹⁴⁻¹⁷ The adsorbed ligands amount is compatible with a single layer coverage (cf. SI, page S4), multilayer adsorption is discarded according to previously reported ligand adsorption isotherms on MWCNTs, showing a simple Langmuir-type adsorption behavior.¹⁴

Table 1. Catalytic performances of our catalysts immobilized in a polymeric film on a glassy carbon electrode. Activity of a Pt electrode is reported as reference.

Catalyst	E _{on} ^a (V ^b)	n _e at +0.164 V ^b		Mass Activity ^c mA/mg _{PGM} ^d
		RRDE	RDE(K.L.) ^c	
MWCNT/HL1-Pd(II)	0.91	3.64	3.51 _{R²=0.999}	173
MWCNT/HL2-Pd(II)	0.95	3.78	3.70 _{R²=0.999}	493
Pt-electrode	0.91		4.10 _{R²=0.999}	

^a Details on E_{on} determination are given in the SI (Figure S1) ^b vs RHE; ^c Calculations provided in Table S1; ^d at 0.9 V vs. RHE; ^e Koutechy-Levich (K.L.) plots provided in Figure S2.

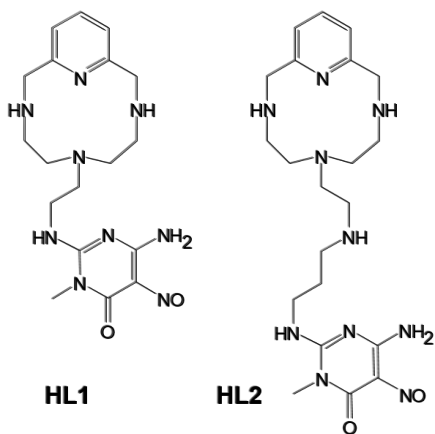


Figure 1. The ligands HL1 and HL2.

Complexation of Pd(II) to the surface azamacrocyclic functionalities of these materials at pH 5.0 afforded the final catalysts MWCNT/HL1-Pd(II) and MWCNT/HL2-Pd(II), possessing a homogeneous distribution of discrete Pd(II) ions at the surface. Such complexes possess an activated position in the cation's first coordination sphere, consisting in an ancillary chloride ligand, as previously reported for analogous systems¹⁴ and re-verified in the present case through XPS (Figure S3) and SEM-EDS analysis (Figure S4). Characterization and stability of the complexes under ORR conditions (pH, potential range) are reported in the SI. Previous reports substantiated the tendency of HL1 to flatten on the CNTs surface upon Pd(II) complexation (moving to MWCNT/HL1 to MWCNT/HL1-Pd(II) reduces BET surface area), while this is not observed for HL2 (moving to MWCNT/HL2 to MWCNT/HL2-Pd(II) has almost no effect on BET surface area). This was ascribed both to the higher loss of degrees of freedom required for the folding of the longer spacer arm back on the surface and to its increased hydrophilicity due to protonation of the extra amino group ($pK_a = 7.51(6)$, working pH 5.0).¹⁴

Samples were prepared according to described methodologies.¹⁴ Details of catalyst preparation are given in the SI. The final Pd content in the catalysts was assessed as 0.242 mmol Pd/g MWCNT/HL1 and 0.258 mmol Pd/g MWCNT/HL2 respectively.

The electrocatalytic performances of these catalysts towards ORR were evaluated in alkaline aqueous solution (0.1 M KOH), by CV. Electrochemical measurements were performed using a three-electrode cell consisting of an Ag/AgCl/sat. KCl reference electrode, a Pt counterelectrode and either a rotating disk electrode (RDE) or a rotating ring disk electrode (RRDE). Immobilization of the catalysts on the working electrode was achieved by preparing an ink for each functionalized sample, consisting of the Pd(II)-functionalized MWCNTs dispersed in a polymeric membrane (Nafion®), which was then casted on a rotating glassy carbon (GC) electrode. Samples were prepared according to reported procedures:¹⁸ a detailed description is available in the SI. A commercial Metrohm Pt-polycrystalline electrode (ϕ 3 mm) was employed to benchmark the performances of our catalysts.

Figure 2 shows the ORR polarization curves recorded at 1600 rpm for each sample at a potential scan rate of 5 mV s⁻¹. Polarization curves for the bare GC electrode, as well as for the GC electrode functionalized with the same strategy with pristine MWCNTs, MWCNT/HL1, MWCNT/HL2 and MWCNT/K₂PdCl₄ are also reported. Relevant data on each electrode performances are given in the SI (Table S2). Preparation and characterization of MWCNT/K₂PdCl₄, where Pd species are directly adsorbed on MWCNTs due to C π -d π interactions,¹⁹ are provided in the SI. During the RRDE CV measurements, the Pt ring-electrode was

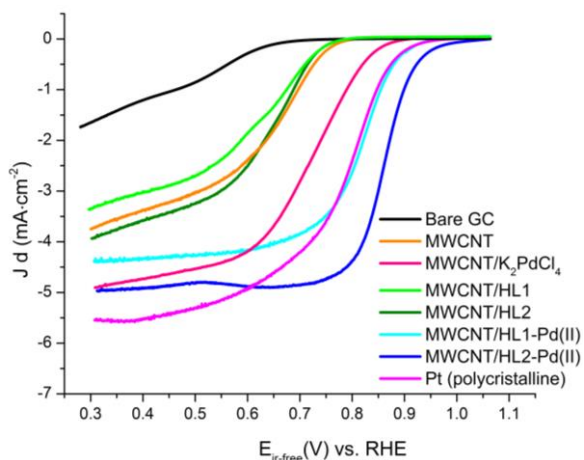


Figure 2. RRDE disk currents showing the O.R.R. activities of the investigated catalysts. Rotation rate: 1600 rpm. Scanning rate: 5 mVs⁻¹.

held at a potential of + 0.50 V vs. Ag/AgCl/sat. KCl to ensure the complete oxidation of H₂O₂ eventually produced at the sample-GC Disk electrode. All electrochemical profiles, background currents (under N₂-saturated conditions) are subtracted from respective curves to remove capacitive contributions (Figure S5). Catalytic activities, both in terms of E_{on} and current values, increase depending on the catalyst nature in the order: bare GC < pristine MWCNTs \approx MWCNT/HL1 \approx MWCNT/HL2 < MWCNT/K₂PdCl₄ < MWCNT/HL1-Pd(II) < MWCNT/HL2-Pd(II). This rules out significant catalytic properties of the substrate and of CNT-supported ligands in our case, while it highlights the prominent role of Pd(II), and of the ligands in enhancing its catalytic activity. Table S2 collects electrochemical parameters for all systems.

As displayed in Figure 2, E_{on} values observed for MWCNT/HL1-Pd(II) and MWCNT/HL2-Pd(II) catalysts are very close to the benchmark values determined in the same conditions with a commercial Pt working electrode. Data in Table 1 reveal that in the case of MWCNT/HL2-Pd(II) the E_{on} value is even better (i.e. more positive) than that observed for the Pt electrode.

The number of exchanged electrons per O₂ molecule is invariably very close to 4, signifying an almost exclusive conversion of O₂ into water. Interestingly, very close values are found either by direct evaluation with RRDE or by extrapolation of Rotating Disk Electrode polarization curves through the Koutechy-Levich (K.L.) equation²⁰⁻²² (Table 1). For this purpose, ORR polarization curves were recorded from 400 to 2000 rpm (step of 400 rpm) with a potential scan rate of 20 mV s⁻¹ (Figure S6). Sample LSV at different scan rate (200 mV/s) are reported in Figure S7. Close convergence of RRDE and K.L. extrapolated data for exchanged electron number suggests high homogeneity of the electrode surface. SEM images of electrode surface are displayed in Figure S8. Measured ring and disk currents for MWCNT/HL2 at the suggested potential of 0.9 V vs RHE demonstrate that in said conditions direct conversion to water efficiency increases, reaching 96.5%; full dependence of ne⁻ vs voltage for Pd-containing catalysts is presented in Figure S9.

Mass activity-wise, both catalysts show satisfactory results, with MWCNT/HL1-Pd(II) reaching 173 mA/mgPd and MWCNT/HL2-Pd(II) scoring 493 mA/mgPd (Table 1).

Although other strategies based on Pd-species are reported, involving either metallic thin film electrodes²³ or Pd(0) nanoparticles (NPs) immobilized onto heteroatom-doped carbon surfaces,²⁴⁻²⁷ this feat of mass activity was only made possible by the careful

design of catalysts to achieve supported discrete ions. As pointed out elsewhere,²⁸ single atoms catalysts would be the ultimate way to maximize the mass/atom activity of PGM metals. Moving from randomly doped systems towards supported discrete macrocyclic complexes with a well-defined chemical identity is a mandatory step in that direction.

XPS spectra of the as-prepared catalysts, reported in Figure 3a, show that all Pd is present as a Pd(II) complex. Ink preparation and subsequent ORR assays do not tamper much the nanostructure of the catalyst, as proved by the complete preservation of features in the C 1s region. Pd does not change its oxidation number upon use of the catalysts, i.e. all Pd remains as Pd(II). After use, new small peaks appear (Figure 3b), which do not change during at least 1000 cycles (Figure S11) and are consistent with formation of either PdO²⁹ or clusters of Pd with surface oxy/hydroxyl groups²⁰ (Figure 3), while most of the metal is still bound to the ligand, demonstrating that we really are in the presence of Pd(II)-complexes active sites. Indeed, TEM images (Figure S10) show the presence of tiny localized traces of NPs, which cannot justify the observed activity. Also, the slight shift in B.E. of the Pd 3d signals and the lack of the chlorine peak in the used catalysts, suggest that the original ancillary chloride ligand was shed in favor of a hydroxide anion. Binding and activation (i.e. for proton exchange) of such water-related species under the reversible conditions granted by the strong binding to a tridentate azamacrocycle, is probably the key mechanism subtending to the observed catalytic activity of these Pd(II) complexes.

According to the characterization of the as-prepared and after use catalysts we cannot detect any major difference between MWCNTs/HL1-Pd(II) and MWCNTs/HL2-Pd(II) either in overall composition, metal oxidation state or Pd(II) coordination environment. For these reasons we are led to think that the longer spacer of HL2, protruding from the MWCNTs surface, either produces a brush-like arrangement of catalytic sites, better suited for capturing gaseous reagents from the solution, or that it promotes a cooperative mechanism involving two neighboring Pd(II) centers.

Stability of catalysts has also been addressed. Concerning Pd leakage, SEM-EDS analysis of the fresh and after use (1000 cycles) MWCNT/HL2 catalysts show the same % abundance of Pd in both samples (Figure S4). The presence of Pd in the electrolyte solution was also checked by ICP-MS after 1000 CV scans, revealing no traces of the metal. Preliminary data indicate that our most promising catalyst, MWCNT/HL2-Pd(II), is able to maintain its performances over time, with no bias observed for produced current density or exchanged electron numbers per O₂ molecule over a 1.5 h test in galvanostatic operating conditions (i.e. simulating a working fuel cell) at -0.80 V vs Ag/AgCl/sat. KCl (Figure S12). Moreover, catalytic performances are also maintained over 1000 CV scans at 200 mV/s (Figure S13). Nevertheless, further investigation is needed to evaluate the long-term stability of the catalyst for fuel cell applications.

In conclusion, herein we reported novel Pd(II) catalysts for ORR, one of which exhibits a half-cell PGM mass activity exceeding state-of-the-art reference goals. Both systems feature E_{on} values comparable or better than that of a commercial Pt electrode and a predominating (90% or above, cf. Figure S9) 4 e⁻ process, leading to the direct production of H₂O. Furthermore, we demonstrated that beyond Pd(0) species, also Pd(II) complexes are feasible as active sites for ORR catalysts. Granted that working mechanism will be the object of upcoming studies, its understanding, together with the good stability displayed by the developed catalysts, foreshadows their rapid put in practice and evaluation in a complete fuel cell. For the reasons above, we strongly believe that these findings will prompt further studies and developments towards

affordable cost-effective solutions for the renewable energetic technology of the immediate future.

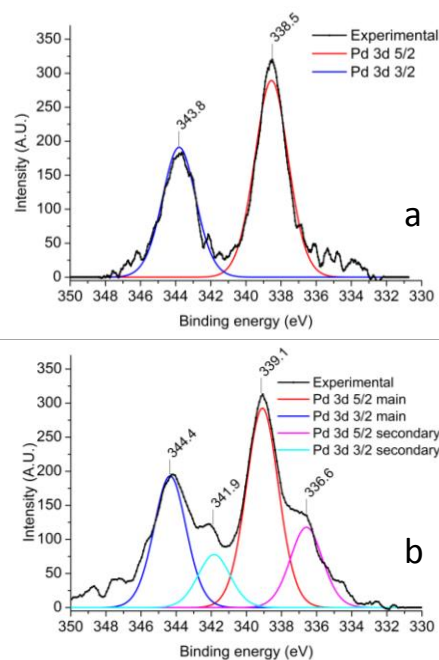


Figure 3. High resolution XPS spectra in the Pd 3d region of a) the as prepared MWCNT/HL2-Pd(II) catalyst and b) of the MWCNT/HL2-Pd(II) GC electrode after use (1 CV from 0.1 V to -0.85 V vs Ag/AgCl/sat. KCl).

ASSOCIATED CONTENT

Supporting Information

Supporting Information is available free of charge on the ACS Publications website.

Synthetic procedures, preparation of modified electrodes, details of Mass Activity Calculation, details and definition of electrochemical measurements and stability tests, SEM-EDS and XPS analyses of MWCNT/HL2-Pd(II) as prepared and after use, still CVs in KOH 0.1 M solutions saturated with N₂/O₂ for both catalysts, linear sweep voltammograms at different spin rates at 20 mV/s scan rate for both catalysts, Koutecky-Levich plots at -0.80 V vs Ag/AgCl/sat. KCl, TEM images of after-use MWCNT/HL2-Pd(II).

AUTHOR INFORMATION

Corresponding Author

*antonio.bianchi@unifi.it
 *enrique.garcia-es@uv.es
 *m.innocenti@unifi.it

Author Contributions

‡ M.P. and M.S. contributed equally.

Notes

The authors declare no competing financial interests.

ACKNOWLEDGMENT

Financial support from the Italian MIUR (project 2015MP34H3), the Spanish Ministerio de Economía y Competitividad (Project CTQ2016-78499-C6-1-R and Unidad de Excelencia MDM 2015-0038) and Generalitat Valenciana (Project PROMETEOII2015-002) is gratefully acknowledged.

REFERENCES

- Morožan, A.; Joussetme, B.; Palacin, S. Low-platinum and platinum-free catalysts for the oxygen reduction reaction at fuel cell cathodes. *Energy Environ. Sci.* **2011**, *4*, 1238–1254.
- Zheng, Y.; Jiao, Y.; Jaroniec, M.; Jin, Y. G.; Qiao, S. Z. Nanostructured metal-free electrochemical catalysts for highly efficient oxygen reduction. *Small* **2012**, *8*, 3550–3566.
- Zhu, C. Z.; Dong, S. J. Recent progress in graphene-based nanomaterials as advanced electrocatalysts towards oxygen reduction reaction. *Nanoscale* **2013**, *5*, 1753–1767.
- Wang, D.-W.; Su, D. Heterogeneous nanocarbon materials for oxygen reduction reaction. *Energy Environ. Sci.* **2014**, *7*, 576–591.
- Yu, D.; Nagelli, E.; Du, F.; Dai, L. Metal-Free Carbon Nanomaterials Become More Active than Metal Catalysts and Last Longer. *J. Phys. Chem. Lett.* **2010**, *1*, 2165–2173.
- Song, C.; Zhang, J. Electrocatalytic Oxygen Reduction Reaction. In *PEM Fuel Cell Electrocatalysts and Catalyst Layers: Fundamentals and Applications*; Zhang, J., Ed.; Springer: New York, **2008**; pp 89–134.
- US Department of Energy: Office of Energy Efficiency and Renewable Energy. <https://www.energy.gov/eere/fuelcells/doe-technical-targets-polymer-electrolyte-membrane-fuel-cell-components>
- Kocha, S. S.; Shinozaki, K.; Zack, J. W.; Myers, D. J.; Kariuki, N. N.; Nowicki, T.; Stamenkovic, V.; Kang, Y.; Li, D.; Papageorgopoulos, D. Best Practices and Testing Protocols for Benchmarking ORR Activities of Fuel Cell Electrocatalysts Using Rotating Disk Electrode. *Electrocatalysis* **2017**, *8*(4), 366–374.
- Shao, M.; Chang, Q.; Dodelet, J.-P.; Chenitz R. Recent Advances in Electrocatalysts for Oxygen Reduction Reaction. *Chem. Rev.* **2016**, *116* (6), 3594–3657.
- Wang, L.; Bellini, M.; Miller, H. A.; Varcoe, J. R. A high conductivity ultrathin anion-exchange membrane with 500+ h alkali stability for use in alkaline membrane fuel cells that can achieve 2 W cm^{-2} at $80 \text{ }^\circ\text{C}$. *J. Mater. Chem. A*, **2018**, *6*, 15404–15412.
- Omasta, T. J.; Peng, X.; Miller, H. A.; Vizza, F.; Wang, L.; Varcoe, J. R.; Dekel, D. R.; Mustain, W. E. Beyond 1.0 W cm^{-2} Performance without Platinum: The Beginning of a New Era in Anion Exchange Membrane Fuel Cells. *J. Electrochem. Soc.* **2018**, *165*, J3039–J3044.
- Miller, H. A.; Lavacchi, A.; Vizza, F.; Marelli, M.; Di Benedetto, F.; D'Acapito, F.; Paska, Y.; Page, P.; Dekel, D. R. A Pd/C-CeO₂ Anode Catalyst for High-Performance Platinum-Free Anion Exchange Membrane Fuel Cells. *Angew. Chem. Int. Ed.* **2016**, *55*, 6004–6007.
- Serp, P.; Machado, B.; *Nanostructured Carbon Materials for Catalysis*; RSC Catalysis Series No. 23; The Royal Society of Chemistry: Cambridge, **2015**; Chapter 7, 370–375.
- Savastano, M.; Arranz-Mascarós, P.; Bazzicalupi, C.; Clares, M.P.; Godino-Salido, M.L.; Gutiérrez-Valero, M.D.; Inclán, M.; Bianchi, A.; García-España, E.; López-Garzón, R. Construction of green nanostructured heterogeneous catalysts via non-covalent surface decoration of multi-walled carbon nanotubes with Pd(II) complexes of azamacrocycles. *J. Catal.* **2017**, *353*, pp. 239–249.
- Savastano, M.; Arranz-Mascarós, P.; Bazzicalupi, C.; Clares, M.P.; Godino-Salido, M.L.; Guijarro, L.; Gutiérrez-Valero, M.D.; Bianchi, A.; García-España, E.; López-Garzón, R. Polyfunctional Tetraaza-Macrocyclic Ligands: Zn(II), Cu(II) Binding and Formation of Hybrid Materials with Multiwalled Carbon Nanotubes. *ACS Omega* **2017**, *2* (7), pp. 3868–3877.
- López-Garzón, R.; Godino-Salido, M. L.; Gutiérrez-Valero, M. D.; Arranz-Mascarós, P.; Melguizo, M.; García, C.; Domingo-García, M.; López-Garzón, F. J. Supramolecular assembling of molecular ion-ligands on graphite-based solid materials directed to specific binding of metal ions. *Inorg. Chim. Acta* **2014**, *47*, 208–221.
- Godino-Salido, M. L.; López-Garzón, R.; Gutiérrez-Valero, M. D.; Arranz-Mascarós, P.; Melguizo-Guijarro, M.; López de la Torre, M. D.; Gómez-Serrano, V.; Alexandre-Franco, M.; Lozano-Castelló, D.; Cazorla-Amorós, D.; Domingo-García, M. Effect of the surface chemical groups of activated carbons on their surface adsorptivity to aromatic adsorbates based on π - π interactions. *Mater. Chem. Phys.* **2014**, *143* (3), 1489–1499.
- Miller, H.A.; Bellini, M.; Oberhauser, W.; Deng, X.; Chen, H.; He, Q.; Passaponti, M.; Innocenti, M.; Yang, R.; Sun, F.; Jiang, Z.; Vizza, F. Heat treated carbon supported iron(ii)phthalocyanine oxygen reduction catalysts: elucidation of the structure-activity relationship using X-ray absorption spectroscopy. *Phys. Chem. Chem. Phys.* **2016**, *18*, 33142–33151.
- Savastano, M.; Arranz-Mascarós, P.; Bazzicalupi, C.; Bianchi, A.; Giorgi C.; Godino-Salido, M. L.; Gutiérrez-Valero, M. D.; López-Garzón R. Binding and removal of octahedral, tetrahedral, square planar and linear anions in water by means of activated carbon functionalized with a pyrimidine-based anion receptor. *RSC Adv.*, **2014**, *4*, 58505–58513.
- Arrigo, R.; Schuster, M. E.; Xie, Z.; Yi, Y.; Wowsnick, G.; Sun, L. L.; Hermann, K. E.; Friedrich, M.; Kast, P.; Havecker, M.; Knop-Gericke, A.; Schlögl, R. Nature of the N–Pd Interaction in Nitrogen-Doped Carbon Nanotube Catalysts. *ACS Catal* **2015**, *5*, 2740–2753.
- Wang, Y.; Zhang, D.; Liu, H. A study of the catalysis of cobalt hydroxide towards the oxygen reduction in alkaline media. *J. Power Sources* **2010**, *195*, 3135–3139.
- Teschner, D.; Vass, E.; Havecker, M.; Zafeiratos, S.; Schnorch, P.; Sauer, H.; Knop-Gericke, A.; Schlögl, R.; Chamam, M.; Wootsch, A. Alkyne hydrogenation over Pd catalysts: A new paradigm. *J. Catal.* **2006**, *242*, 26–37.
- Tsui, L.; Zafferoni, C.; Lavacchi, A.; Innocenti, M.; Vizza, F.; Zangari, G. Electrocatalytic activity and operational stability of electrodeposited Pd–Co films towards ethanol oxidation in alkaline electrolytes. *J. Power Sources* **2015**, *293*, 815–822.
- Arrigo, R.; Wrabetz, S.; Schuster, M. E.; Wang, D.; Villa, A.; Rosenthal, D.; Girschgies, F.; Weinberg, G.; Prati, L.; Schlögl, R.; Su, D. S. Tailoring the morphology of Pd nanoparticles on CNTs by nitrogen and oxygen functionalization. *Phys. Chem. Chem. Phys.* **2012**, *14*, 10523–10532.
- Arrigo, R.; Schuster, M. E.; Abate, S.; Wrabetz, W.; Amakawa, K.; Teschner, D.; Freni, M.; Centi, G.; Perathoner, S.; Havecker, M.; Schlögl, R. Dynamics of palladium on nanocarbon in the direct synthesis of H₂O₂. *ChemSusChem* **2014**, *7*, 179–194.
- Bard, A. J.; Faulkner, L. R. *Electrochemical Methods: Fundamentals and Applications*, 2nd ed.; John Wiley & Sons, Inc.: New York, **2001**; p 856.
- Wang, L.; Lavacchi, A.; Bevilacqua, M.; Bellini, M.; Fornasiero, P.; Filippi, J.; Innocenti, M.; Marchionni, A.; Miller, H. A.; Vizza, F. Energy Efficiency of Alkaline Direct Ethanol Fuel Cells Employing Nanostructured Palladium Electrocatalysts. *ChemCatChem* **2015**, *7*, 2214–2221.
- Liu, J. Catalysis by Supported Single Metal Atoms. *ACS Catal.*, **2017**, *7* (1), pp 34–59.
- Wua, Q.; Rao, Z.; Yuan, L.; Jiang, L.; Sun, G.; Ruan, J.; Zhou, Z.; Sang, S. Carbon supported PdO with improved activity and stability for oxygen reduction reaction in alkaline solution *Electrochim. Acta*, **2014**, *150*, 157–166.

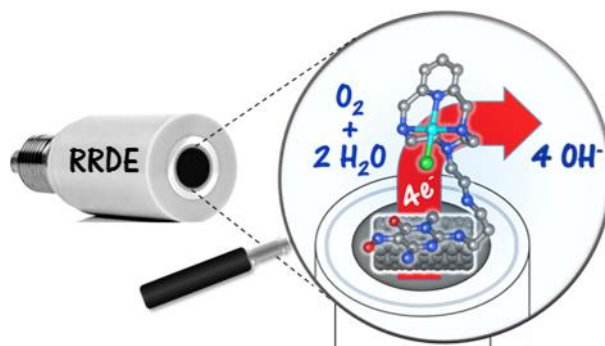


Table of Contents Synopsis

Two new Pd(II) catalysts supported on MWCNTs exhibit very efficient catalytic activity toward oxygen reduction reactions (ORR) in alkaline solution. Both systems feature E_{on} values comparable or better than that of a commercial Pt electrode and almost quantitative conversion of O_2 to H_2O (4 e- process). One of them gives a half-cell PGM mass activity exceeding state-of-the-art reference goals.